7-1980

Ultrasonic Detection of Surface Flaws in Gas Turbine Ceramics

Thomas Derkacs
Thompson-Ramo-Wooldridge

I. M. Matay
Thompson-Ramo-Woolridge

Ultrasonic Detection of Surface Flaws in Gas Turbine Ceramics

Abstract
This paper presents the results of a program sponsored by NADC for NASC to develop an ultrasonic surface wave technique for detection of small flaws, <100 11m>(< 0.004 inch), in gas turbine quality ceramics. A 45 MHz ultrasonic surface wave inspection technique is described, which employs immersion scanning ndd C-scan recording. Inspection results are presented using this technique on specimens of hot pressed Silicon nitride and silicon carbide, from two sources each, and reaction bonded silicon nitride. Results are also presented of four-point-bend tests and scanning electron micrography, which were used to identify defect sizes and types and to correlate flexural strength with inspection results. The flexural strength is shown to correlate, at least qualitatively, with the extent of ultrasonic response from machining damage. The sensitivity to individual defects is shown to be limited primarily by the extent of machining damage and the spot size of the ultrasonic beam.

Keywords
Nondestructive Evaluation

Disciplines
Materials Science and Engineering

ULTRASONIC DETECTION OF SURFACE FLAWS IN GAS TURBINE CERAMICS

T. Derkacs and I. M. Matay
TRW, Inc.
TRW Materials Technology
Cleveland, OH 44117

ABSTRACT

This paper presents the results of a program sponsored by NADC for NASC to develop an ultrasonic surface wave technique for detection of small flaws, <100 μm (< 0.004 inch), in gas turbine quality ceramics. A 45 MHz ultrasonic surface wave inspection technique is described, which employs immersion scanning and C-scan recording. Inspection results are presented using this technique on specimens of hot pressed silicon nitride and silicon carbide, from two sources each, and reaction bonded silicon nitride. Results are also presented of four-point-bend tests and scanning electron micrography, which were used to identify defect sizes and types and to correlate flexural strength with inspection results. The flexural strength is shown to correlate, at least qualitatively, with the extent of ultrasonic response from machining damage. The sensitivity to individual defects is shown to be limited primarily by the extent of machining damage and the spot size of the ultrasonic beam.

INTRODUCTION

This paper describes a program sponsored by the NADC for the NASC to develop a very high frequency (VHF) surface wave inspection technique for gas turbine ceramics. In earlier programs we developed a longitudinal wave technique (Ref. 1) capable of detecting defects down to at least 0.001 inches (25 μm) in size with a near-surface deadband of 0.0063 inches (160 μm), and a shear wave technique (Ref. 2) that improved the sensitivity so that 0.0004 inch (10 μm) defects can be detected, and reduced the near-surface deadband to 0.0016 inches (40 μm). The purpose of this program (Ref. 3) was to develop a near-surface inspection technique in order to eliminate the remaining deadband. As in the earlier programs, our approach for surface defects was to develop a technique that would allow scanning of a reasonable volume of material in a practical period of time. Our goal was to develop an immersion technique in order to allow rapid scanning and automatic data recording so that the combination of the three techniques, longitudinal, shear and surface waves, would allow an automated inspection providing complete part coverage.

TECHNIQUE

Ultrasonic surface wave inspection at conventional frequencies is normally a manual, contact operation in which no provision is made to automatically correlate defects with their locations in the part. This is necessary because immersion testing is not usually possible. A surface wave traveling on a part submerged in water radiates energy into the water and quickly dissipates. The method used in this program to overcome this limitation is illustrated in Fig. 1. The transducer used was an Aerotech Laboratories 45 MHz alpha transducer with a focal length of 1.8 inches in water and a beam spot size at half-amplitude of .023 inches (580 μm). The transducer and part were submerged in water and the transducer was tilted at an angle to the entry surface of about 18^{o} in order to generate surface waves in the specimen by mode conversion. The water path was set so that the beam was focused in the material a short distance past the point of entry. This provides the shortest possible path length and therefore the minimum possible loss in a reflected pulse from a surface defect. The ultrasonic defect gate was set to encompass only the transducer focal point, so that as the transducer was scanned over the part a defect indication was recorded only when the beam was focused on the defect.

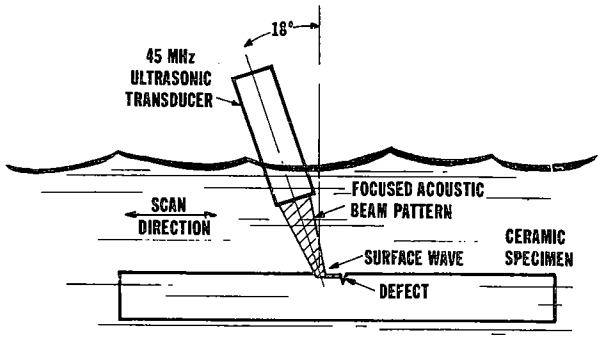

Fig. 1 Immersion 45 MHz Ultrasonic Surface Wave Technique.

INSPECTIONS

Initial evaluations were performed to demonstrate that the technique does indeed generate surface waves. A simple test was to make a recognizable mark, such as a number or letter, on the surface of a ceramic specimen with a grease pencil. Then when the part was inspected, the mark showed up as a defect indication. This technique points out the importance of cleanliness. Any air bubble or dust particle on the part surface shows up as a defect indication. We adopted the policy of individually checking significant defect indications by brushing the surface to make sure the "defect" could not be removed. A more sophisticated technique for ensuring the presence of surface waves was to inspect a billet to locate surface flaws and then to machine off a thin layer and re-inspect the part. Figures 2 and 3 show an example of this technique. Figure

2 shows a C-scan recording of a 45 MHz ultrasonic surface wave inspection of a 7 1/2 inch (19 cm) diameter billet of NC-350 reaction bonded silicon nitride (RBSN). After inspection the billet was cut to remove the three numbered specimens and the left hand side was machined to remove 0.0006 inches (15 μm) in the shaded area. The machining was done to split the linear indication in that portion of the billet. The grinding was perpendicular to the cut edge. Figure 3 shows the same portion of the billet after machining. The linear indication was removed in the machined area while remaining in the unmachined area. It is apparently less than 0.0006 inches (15 μm) deep. The defect indication labelled F was reduced in size but not removed. This defect is apparently greater than 0.0006 inches (15 μm) deep. The inspection technique was also found to be sensitive to machining damage. Figure 4 shows a scan of the same part made parallel to the cut edge and therefore perpendicular to the machining direction. In this case the entire machined area appears defective. This is a significant fact, since it is known that flexural strength specimens ground parallel to their major axis are stronger than those ground perpendicular to their major axis. Figures 3 and 4 indicate that the surface wave technique is sensitive to this difference in grinding direction and therefore to strength.

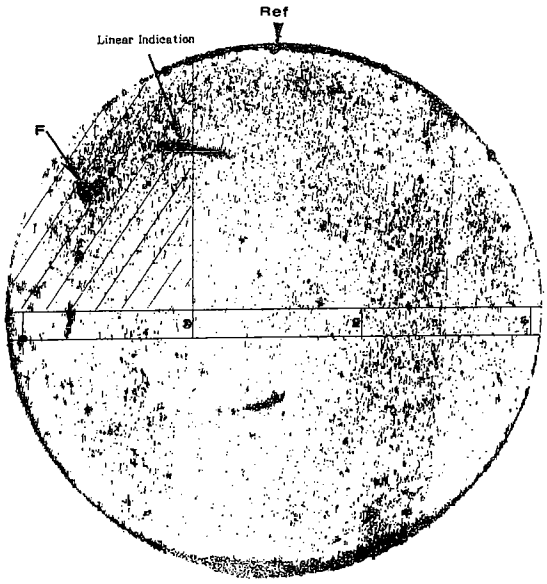

Fig. 2 Machined (Shaded) Area Overlayed on C-Scan Recording of 45 MHz, 18° Surface Wave Inspection of Top Surface of Billet of NC-350 RBSN.

Figures 5, 6 and 7 show another billet that was used to verify the presence of surface waves. This is a billet of Ceralloy 147A hot pressed silicon nitride (HPSN) which was received in the as-pressed condition and then was machined to remove a total of about 0.040 inches (1000 μm) to provide smooth surfaces on both sides. The areas of heavy concentrations of indications in Fig. 5 correspond to the areas shown in the photomacrographs (7X) of Fig. 6 which contain surface ridges left by the pressing operation. After machining these ridges away, the indications in areas A and B disappeared. The billet of Ceralloy 147A HPSN was inspected by both shear and surface waves before machining and by surface waves after machining. A comparison of the before and after surface wave inspections shows no significant correlation in indications. This is to be expected given the amount of material removed. A comparison of the shear wave

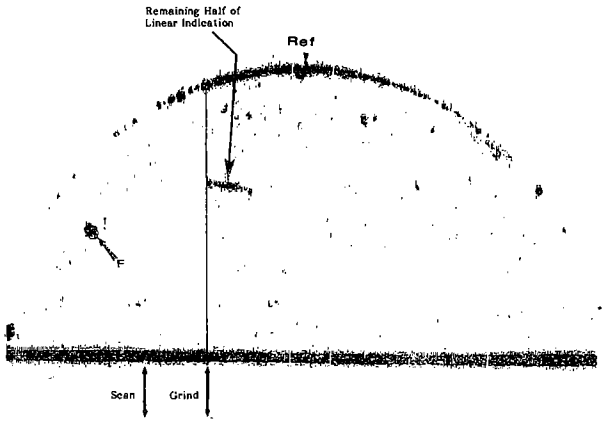

Fig. 3 C-Scan Recording of 45 MHz, 18° Surface Wave Inspection of Top Surface of Segment of Billet of NC-350 RBSN Containing Machined Area (Scan Parallel to Grinding Direction).

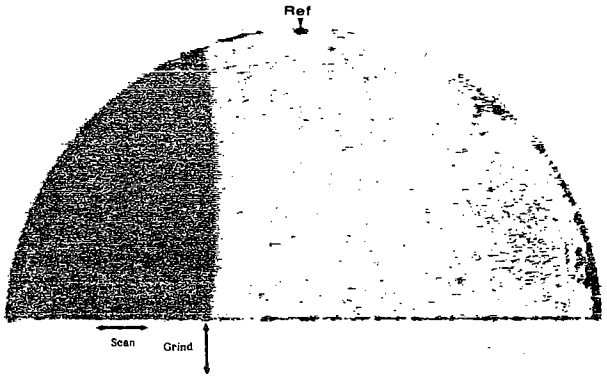

Fig. 4 C-Scan Recording of 45 MHz, 18° Surface Wave Inspection of Top Surface of Segment of Billet of NC-350 RBSN Containing Machined Area (Scan Perpendicular to Grinding Direction).

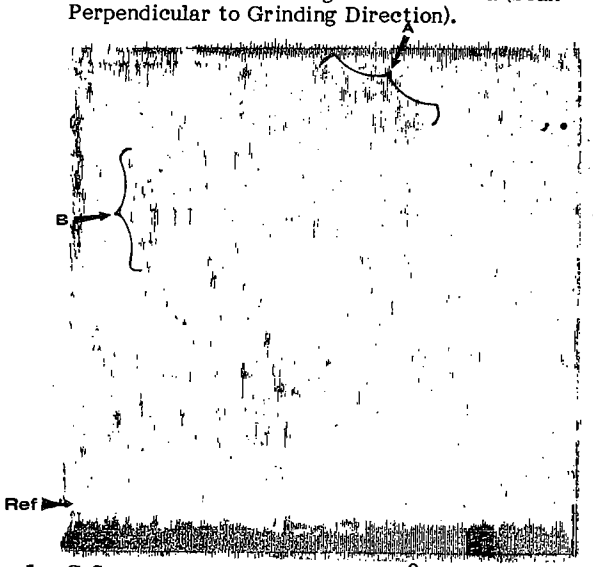

Fig. 5 C-Scan Recording of 45 MHz, 18° Surface Wave Inspection of Billet of Ceralloy 147A Hot Pressed Silicon Nitride (notch up).

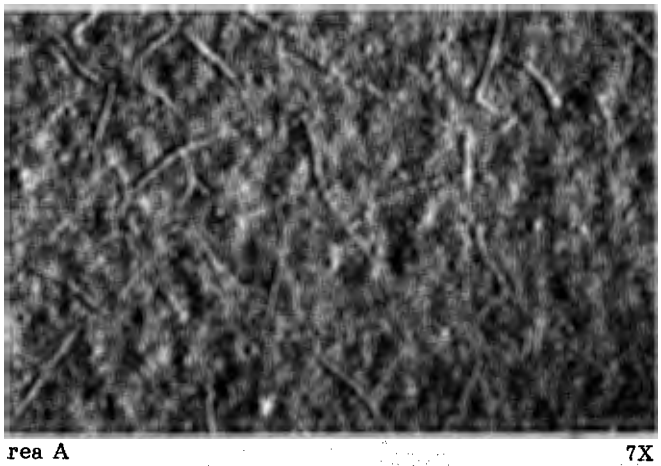

rea A 7X

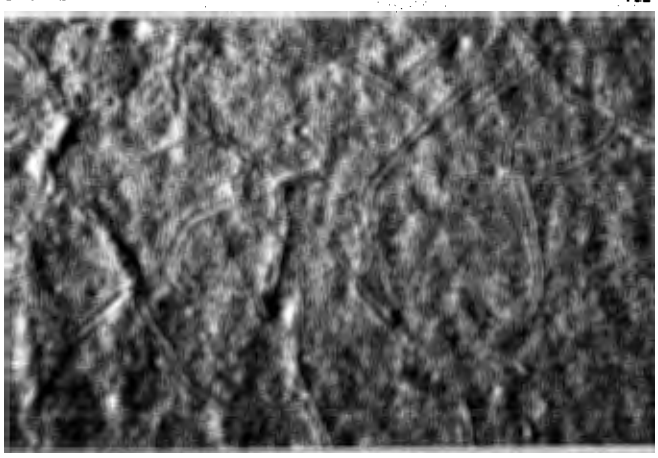

rea B 7X

Fig. 6 Photomacrographs Showing Surface Condition of Two Typical Areas of As-Pressed Billet of Ceralloy 147A HPSN Where Large Numbers of Surface Wave Indications Were Detected.

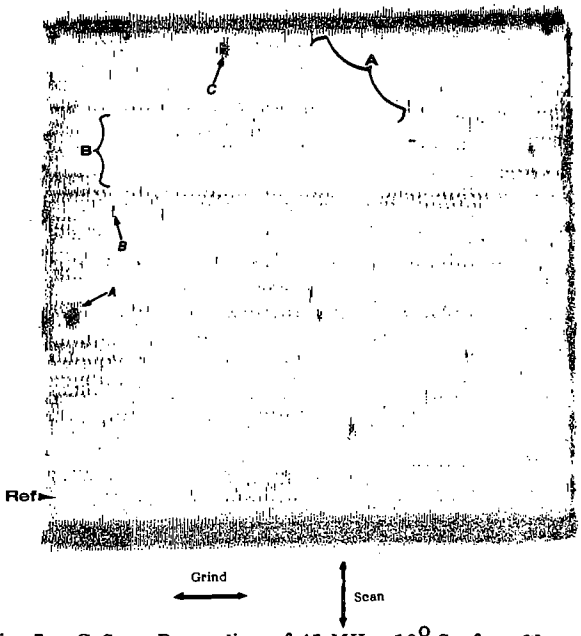

Fig. 7 C-Scan Recording of 45 MHz, 18° Surface Wave Inspection of Top Surface of Billet of Ceralloy 147A HPSN After Machining (Scan Perpendicular to Grinding Direction).

results before machining and the surface wave inspections after machining show a number of corresponding indications. The defects labelled A, B and C in Fig. 7, for example, correspond to defect indications in the corresponding shear wave scan.

Billets of NC-132 and Ceralloy 147A HPSN, NC-350 RBSN, NC-230 and Ceralloy 146 hot pressed silicon carbide (HPSiC) and boron doped sintered SiC were inspected using the surface wave technique. In each case inspections were made on both major surfaces both parallel and perpendicular to the grinding direction. Fig. 7 is the result of a scan made perpendicular to the grinding direction in the billet of Ceralloy 147A HPSN. In this case the sensitivity was reduced so only the most severe grinding damage was detected, thereby allowing the individual defects to also be seen. Figures 8 and 9 show the inspection results for one surface of the billet of NC-132 HPSN. The rectangles in these figures represent four-point-bend specimens machined from this billet. Figure 8 shows a defect-free billet except for very tiny indications in specimens 1, 2 and 3. Figure 9 shows a scan of the same surface perpendicular to the grinding damage. Figure 10 shows the nine bend specimens after machining. This scan was made parallel to the major axis so as to be sensitive to strength controlling defects. The contrast between grinding directions is readily apparent. Similar results were obtained for the other materials tested.

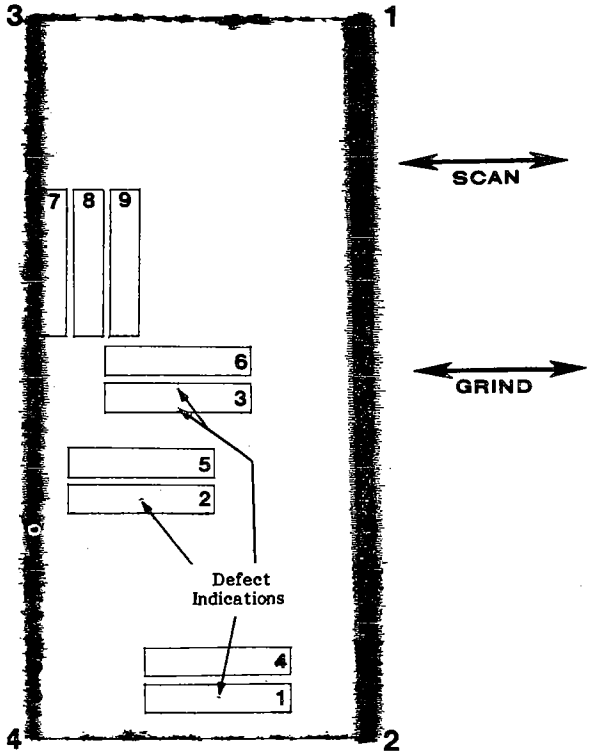

Fig. 8 C-Scan Recording of 45 MHz Ultrasonic Surface Wave Inspection of Bottom of Billet of NC-132 HPSN (Scan Parallel to Grinding Direction).

MECHANICAL TESTING

Four-point-bend specimens were made from each of the billets inspected. Specimens were made from defect free areas machined parallel to the major axis, from areas showing grinding indications as a result of being machined perpendicular to the grinding damage, and from areas containing only individual defect indications. The specimens were machined with a 320 grit diamond wheel

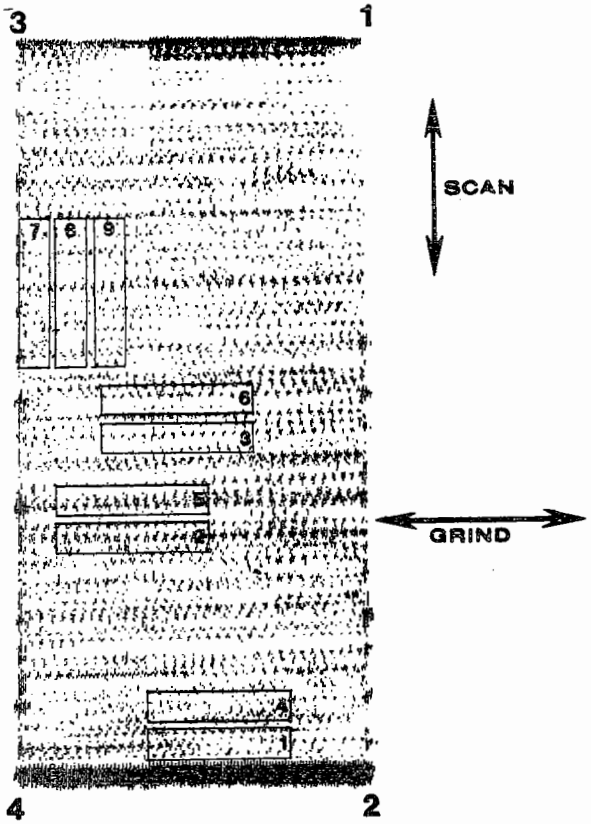

Fig. 9 C-Scan Recording of 45 MHz Ultrasonic Surface Wave Inspection of Bottom Surface of Billet of NC-132 HPSN (Scan Perpendicular to Grinding Direction).

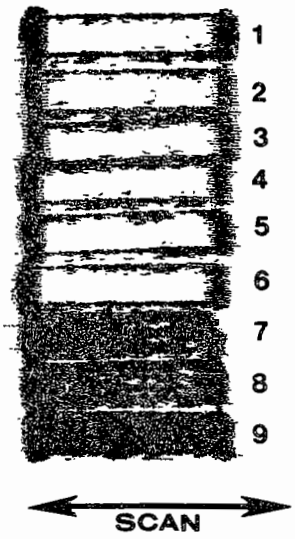

Fig. 10 C-Scan Recording of 45 MHz Ultrasonic Surface Wave Inspection of Tensile Surfaces of NC-132 HPSN Four-Point-Bend Specimens.

parallel to the major axis on all surfaces except the tensile surface, which was left as inspected. The specimens were also chamfered 0.005 inches (125 μm) at 45° on the edges. One specimen of each material machined parallel to the major axis was given a 1 kg Vicker's indentation and one specimen of each machined perpendicular to the major axis was given a 50 kg Vicker's indentation. With the quality of surfaces involved (all billets had originally been machined with a 320 grit diamond wheel) only the 50 kg Vicker's could be resolved ultrasonically.

The four-point-bend tests along with SEM fractography provided data on material strength, fracture origin location with respect to indication location and the nature and size of fracture origins. From this data it was possible to correlate a number of strength limiting defects with their ultrasonic responses. Figures 11 through 16 show some typical ultrasonically detected fracture origins. Figure 11 shows a surface pit in specimen #2 of Ceralloy 147A HPSN. It is about 0.0072" (180 μm) across and 0.0030" (75 μm) deep. Figure 12 shows a typical 50 kg Vicker's indentation; a pit about the same size as in the previous specimen with a crack extending over 0.020 inches (500 μm) deep in the part. Figure 13 shows the 1 kg Vicker's indentation in the same material, an approximately 0.002 inch (60 μm) deep crack. Figure 14 shows a 0.020 inch (500 μm) wide by 0.012 inch (300 μm) deep area of very large grains in specimen #3 of Ceralloy 147A HPSN. Figure 15 shows a flake-like inclusion about 0.0004" (10 μm) thick and 0.0028" (70 μm) wide located 0.0008" (20 μm) below the surface. This is defect A in Fig. 7. Figure 15 shows the smallest defect correlated with an ultrasonic indication, a 0.0006" (16 μm) wide by 0.0008" (20 μm) deep area of large grains at the surface in specimen #1 of NC-132 HPSN (see Fig. 8 for the indication). A defect of about this same size was the largest one found at a fracture origin that could not be correlated with an ultrasonic indication. This suggests that this size defect may not have a high probability of being detected.

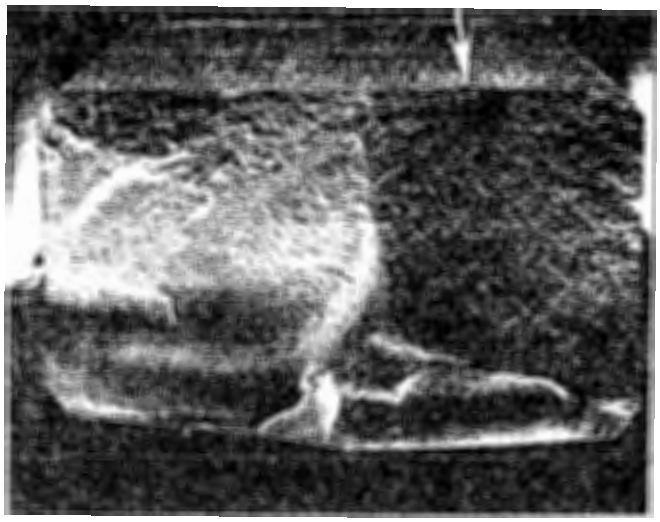

16X

100X

Fig. 11 Fracture Surface of Ceralloy 147A Specimen No. 2 Showing Ultrasonically Detected Surface Pit at Fracture Origin.

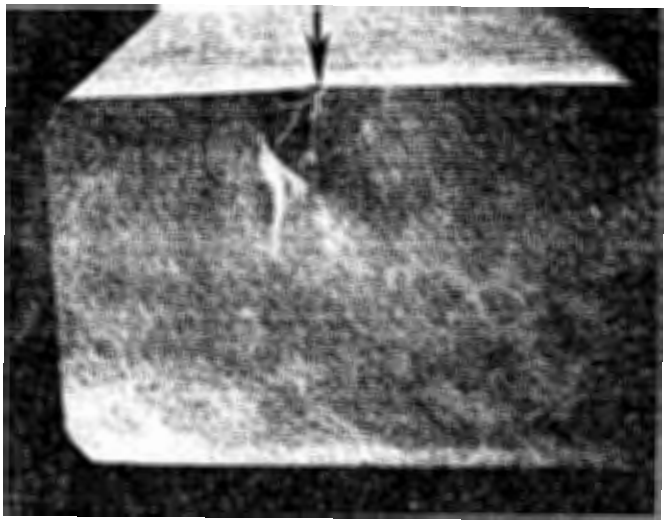

16X

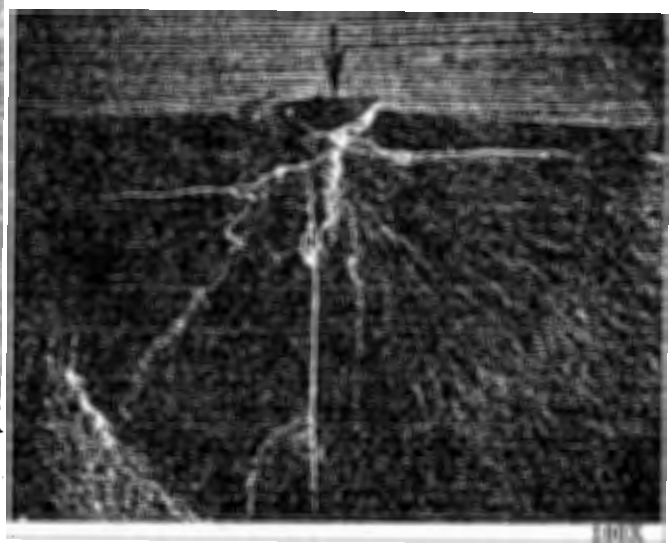

Fig. 12 Fracture Surface of Ceralloy 147A HPSN Specimen No. 9 Showing Fracture Origin at 50 kg Vicker's Indentation.

Based on the strength measurements and SEM analysis, a graph was made of strength versus defect size for the two types of HPSN. This is shown in Fig. 17. The largest defects on the graph are 50 kg Vicker's indentations. The zero defect size is defect free material ground parallel to the major specimen axis. The points in between are ultrasonically detected defects. A graph was also made based on measured strengths parallel and perpendicular to grinding. This is shown in Fig. 18 for two types of HPSN and two types of HPSiC. The ultrasonic response is designated light damage (below a certain threshold) or heavy damage (above a certain threshold). Although the correlation shown in this graph is only qualitative, these results indicate that by assigning a numerical value to the magnitude of ultrasonic response, it may be possible to measure the material strength associated with a given surface finish.

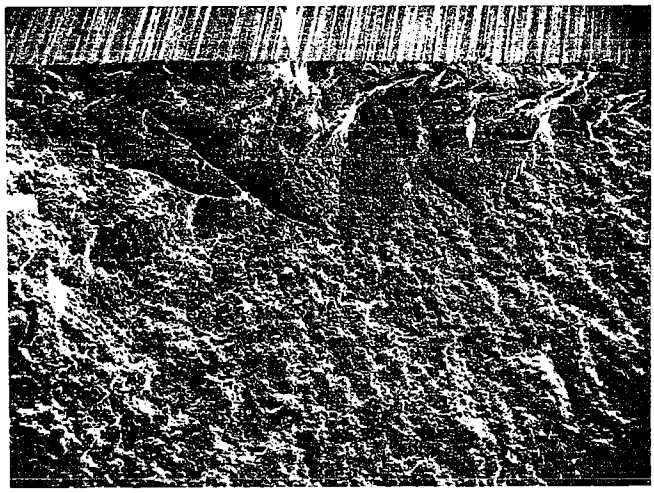

100X

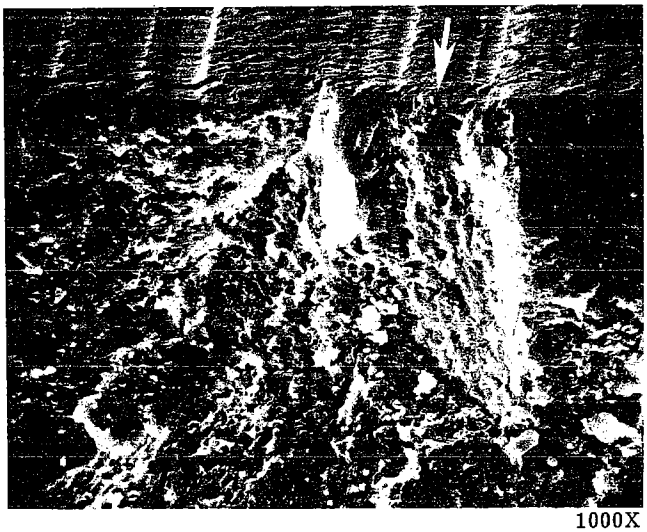

1000X

Fig. 13 Fracture Surface of Ceralloy 147A HPSN Specimen No. 6 Showing Fracture Origin at 1 kg Vicker's Indentation.

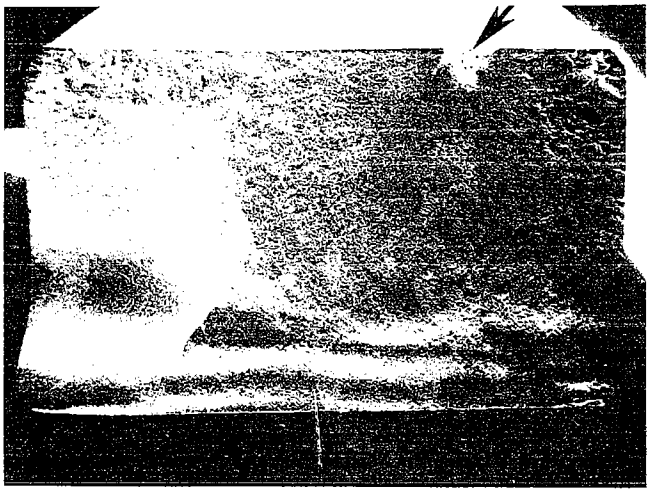

16X

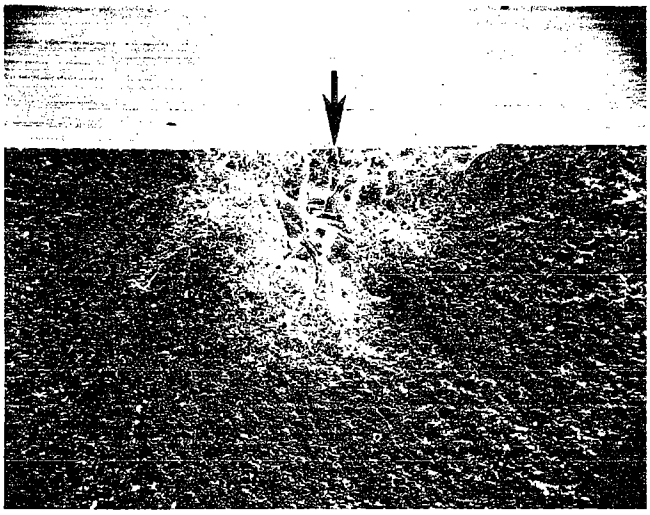

100X

Fig. 14 Fracture Surface of Ceralloy 147A HPSN Specimen No.3 Showing Ultrasonically Detected Fracture Origin.

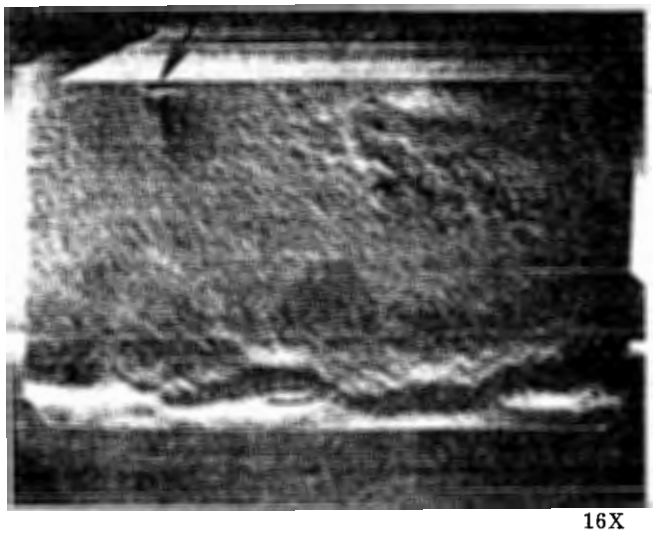

16X

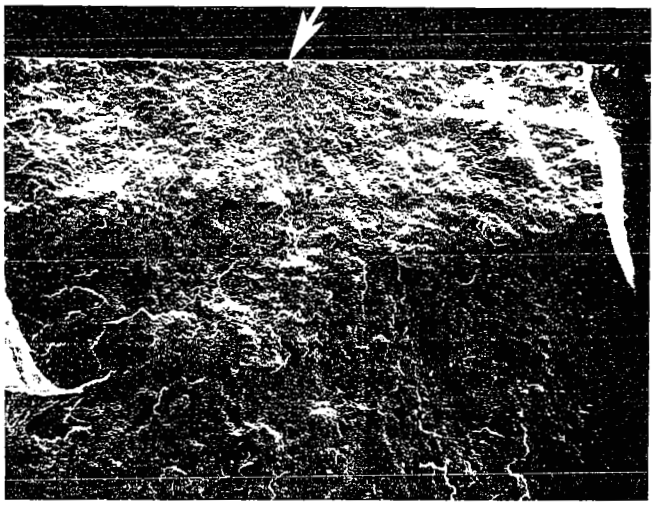

100X

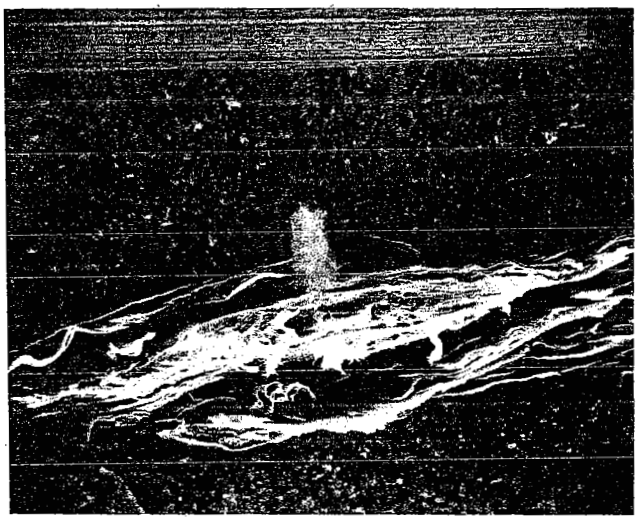

500X

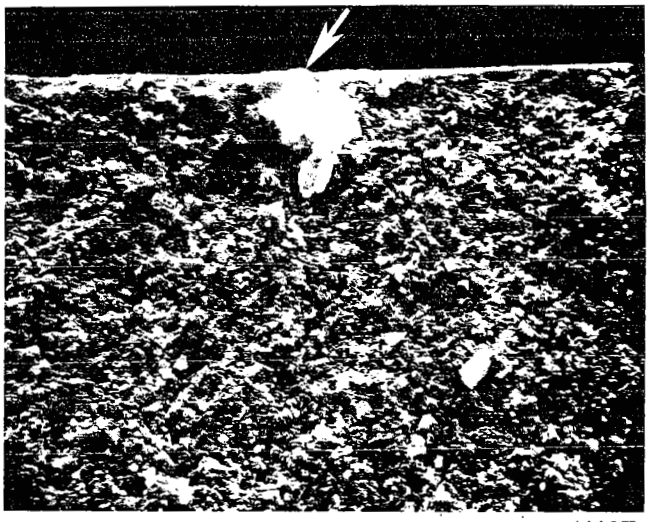

1000X

Fig. 15 Fracture Surface of Ceralloy 147A HPSN Specimen No. 4 Showing Ultrasonically Detected Fracture Origin.

Fig. 16 Fracture Surface of NC-132 HPSN Specimen No. 1 Showing Ultrasonically Detected Fracture Origin.

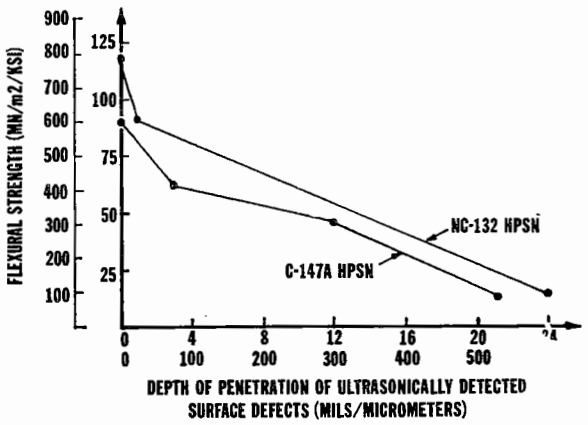

Fig. 17 Flexural Strength as a Function of the Depth of Penetration of Ultrasonically Detected Surface Defects.

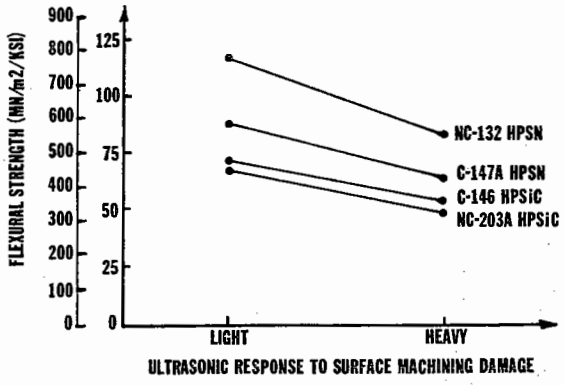

Fig. 18 Flexural Strength as a Function of Ultrasonically Detected Surface Damage in HPSN and HPSiC.

DISCUSSION

The results indicate that, in general, a part may have a general background of machining damage and also individual larger defects. If an individual defect is large enough to be strength limiting, then the inspection technique must be capable of distinguishing it from the background caused by surface damage. A good example of such a defect is the 1 kg Vicker's indentation used in this program. Although the 1 kg indentations could not be detected against the machining background, the specimens containing these indentations were weaker than the other specimens cut parallel to the grinding direction and in some cases were weaker than those cut perpendicular to the grinding direction. Therefore improved discrimination capability is needed to allow detection of the strength limiting defect.

A simple model for estimating discrimination sensitivity is to assume that the reflected pulse from a defect is proportional to the percentage of the beam that it intercepts. Using this assumption, surface damage 0.0006 inches (15 μm) deep would limit defect detection with a 0.023 inch (580 μm) diameter beam to a semi-circular crack 0.0043 inches (108 μm) deep. This assumes that a 3 to 1 signal-to-noise ratio is required for reliable detection. This situation can be improved by either reducing the depth of the machining damage or the diameter of the beam. If the machining damage is reduced to a depth of 0.0002 inches (5 μm), the minimum detectable defect becomes 0.0025 inches (63 μm). If the beam diameter is reduced to 0.005 inches (125 μm), a defect 0.0028 inches (70 μm) deep can be detected. If both are done a defect 0.0016 inches (40 μm) deep can be detected. Although the size of defects calculated may not be accurate because of the simplified assumptions used to calculate them, the numbers illustrate the order of magnitude improvement that is possible.

CONCLUSIONS

Based on the experimental results, the following conclusions can be drawn:

1. A very high frequency (VHF) immersion ultrasonic surface wave inspection technique has been successfully developed;

2. The technique is capable of detecting small defects, penetrating less than 0.001 inch (25 μm) deep in the material;

3. A quantitative correlation has been shown between flexural strength and the depth of ultrasonically detected strength controlling defects;

4. A qualitative correlation has been shown between flexural strength and ultrasonically detected surface damage; and,

5. Sensitivity to individual strength controlling defects is limited by the extent of the machining damage and the ultrasonic beam diameter.

REFERENCES

1. Derkacs, T., Matay, I.M. and Brentnall, W.D., "Nondestructive Evaluation of Ceramics," Final Report, Contract N00019-75-C-0238, Naval Air Systems Command, July 1976, TRW Internal Report No. ER-7798-F.

2. Derkacs, T., Matay, I.M., and Brentnall, W.D., "Ultrasonic Inspection of Ceramics Containing Small Flaws," Final Report, Contract N62269-76-C-0148, Naval Air Development Center for Naval Air Systems Command, August 1977, Internal Report No. ER-7867-F.

3. Derkacs, T. and Matay, I. M., "Detection of Surface Flaws in Gas Turbine Ceramics," Final Report, Contract N62239-C-0136, Naval Air Development Center for Naval Air Systems Command, June 1979, Internal Report No. ER-7980-F.

SUMMARY DISCUSSION
(T. Derkacs)

Wolfgang Sachse (Cornell University): The transducer you used is 45 megahertz?

Tom Derkacs: Yes.

Wolfgang Sachse: Is that a commercial device, or did you --

Tom Derkacs: We bought it commercially. I'm not sure whether it's still available. It was.

John Prati (Teledyne CAE): The C scans you showed, there was a lot of background or things that you didn't pick out and mark as defects. Is this --

Tom Derkacs: In the case of the reaction bonded silicon nitride when you buy it, it has lines in the surface that are caused by cutting in the green state, and those lines are about 15 microns deep. And you do get a background indication from those. If you were to turn it so it actually lines up perpendicular to the beam these lines would cause a black background at this sensitivity. In the scan shown in the slide it was turned at an angle, so we're not getting a strong reflection. It does give a problem of background.

# #